

# Intravascular ultrasonography allows accurate assessment of abdominal aortic aneurysm: An in vitro validation study

Jeroen A. van Essen, MD, Aad van der Lugt, PhD, Elma J. Gussenhoven, PhD, Trude C. Leertouwer, MD, Pieter Zondervan, MD, and Marc R. H. M. van Sambeek, MD, Rotterdam, The Netherlands

**Objective:** The objective of this study was to acquire insight into the interpretation of intravascular ultrasound images of the abdominal aorta and to assess to what extent this technique can provide useful parameters for the endovascular treatment of patients with abdominal aortic aneurysm.

**Study Design:** This was a descriptive study.

**Methods:** Fifteen abdominal aortic specimens (normal, atherosclerotic, or aneurysmal) were studied. Ultrasonic images and corresponding histologic sections were compared for vessel wall characteristics, lesion morphologic characteristics, and lumen diameter. The length of the aneurysm and the length of the proximal and distal neck were measured and compared with external measurements. Tomographic images were reconstructed to a three-dimensional format.

**Results:** Normal aortic wall was seen as a two- or three-layered structure corresponding with intima, media, and adventitia. A distinction could be made among fibrous lesion, calcified lesion, and thrombus and between normal and aneurysmal aorta. Correlation between the histologic specimens and intravascular ultrasonography for lumen diameter measurements was high ( $r = 0.93$ ;  $p < 0.001$ ). In a similar fashion, correlation between external measurements and intravascular ultrasound measurements on the length of the aneurysm and its proximal and distal neck was high ( $r = 0.99$ ;  $p < 0.001$ ). Three-dimensional analysis enhanced interpretation of the tomographic images by visualizing the spatial position of anatomic structures and contributed to understanding the shape and dimensions of the aneurysm.

**Conclusions:** Intravascular ultrasonography provides accurate information on the vessel wall, lesion morphologic characteristics, and quantitative parameters of the abdominal aorta. Spatial information supplied by three-dimensional analysis contributes to a more realistic interpretation of the tomographic images. (J Vasc Surg 1998;27:347-53.)

Since the introduction of the endoluminal stent graft for the treatment of abdominal aortic aneurysm,<sup>1</sup> several studies have demonstrated the feasibility of this therapy.<sup>2-9</sup> This kind of endovascu-

lar intervention depends increasingly on accurate and detailed visualization of the anatomy of the abdominal aorta. Intravascular ultrasonography (IVUS), which permits detailed high-quality imaging of coronary and peripheral vessels,<sup>10-12</sup> may be suitable to provide information before and during endovascular treatment of patients with abdominal aortic aneurysm. This in vitro study was undertaken to acquire insight into the interpretation of IVUS images of normal and diseased abdominal aorta and to examine the accuracy of IVUS-assessed parameters that may be useful during endovascular aneurysm repair.

## METHODS

**Human specimens.** Human aortic specimens removed at autopsy from patients older than 60 years of age at death and classified on external

From the Departments of Cardiology (Drs. van Essen, Gussenhoven, and Leertouwer), Radiology (Dr. van der Lugt), Pathology (Dr. Zondervan), and Vascular Surgery (Dr. van Sambeek) of the University Hospital Rotterdam-Dijkzigt and the Erasmus University Rotterdam.

Supported by grants from the Interuniversity Cardiology Institute, the Netherlands, and the Netherlands Heart Foundation (no. 95.123 and 91.016).

Reprint requests: Elma J. Gussenhoven, PhD, Erasmus University Rotterdam, Department of Echocardiology (Ee 2312), P.O. Box 1738, 3000 DR Rotterdam, the Netherlands.

Copyright © 1998 by The Society for Vascular Surgery and International Society for Cardiovascular Surgery, North American Chapter.

0741-5214/98/\$5.00 + 0 24/1/86416

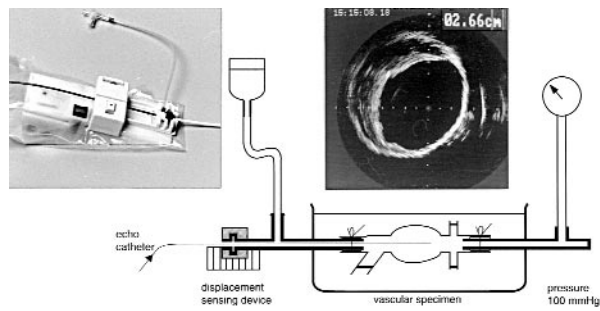


**Fig. 1.** In vitro setup showing intravascular ultrasound catheter advanced through sensing unit of displacement-sensing device and sheath toward pressurized vascular specimen. Catheter tip position in relation to proximal sheath is indicated in **right upper corner**. Displacement-sensing device is seen in insert in **left upper panel**. Calibration: 5 mm.

appearance as normal ( $n = 5$ ), atherosclerotic with calcification ( $n = 5$ ), or aneurysmal (diameter 3.5 to 7 cm,  $n = 5$ ) were studied in vitro. Side branches were tied off with sutures, and the proximal and distal ends were connected to sheaths fixed to a water-bath that was maintained at room temperature. During the study the aorta was pressurized at 100 mm Hg by means of a fluid reservoir containing water connected to the side arm of the distal sheath (Fig. 1). The investigation was approved by the Local Committee on Human Research.

**Intravascular ultrasonography.** Mechanical IVUS systems used were the Microsound system with a Princeps 30 MHz 4.3F catheter (Endosonics, Rijswijk, the Netherlands) and the HP-Sonos Intravascular Imaging System (Hewlett Packard, Andover, Mass.) with a Sonicath Side-Saddle 12.5 MHz 6.2 F catheter (Boston Scientific Corp., Watertown, Mass.). Because the Microsound system permits a maximum radius of 30 mm, this system was used only in normal and atherosclerotic aortas. A displacement-sensing device was used to match IVUS images with corresponding histologic sections, to assess the distance between the major side branches, and to determine the length of the aneurysm and proximal and distal neck; in addition, the displacement-sensing device was used to reconstruct a three-dimensional (3D) image of the aorta.<sup>13</sup> The displacement of the IVUS catheter tip in steps of 0.01 cm was related to the reference site (i.e., the proximal sheath) and was mixed automatically with the ultrasound information on the video screen (Fig. 1). IVUS images were stored on videotape (S-VHS) for further analysis.

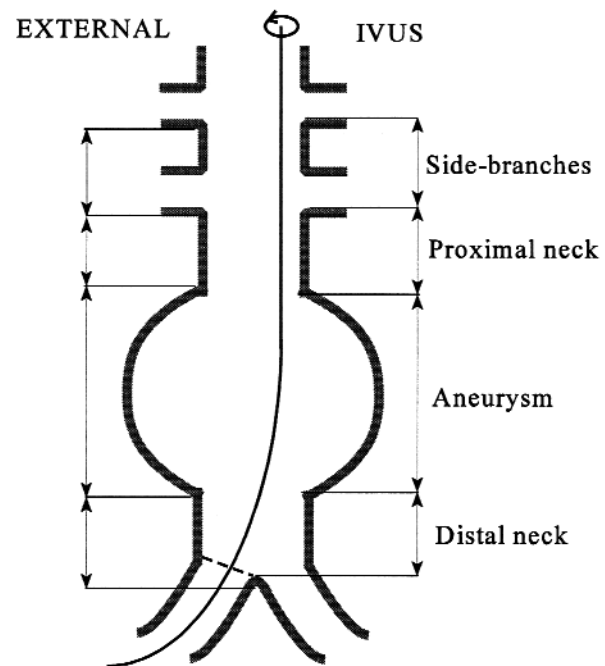


**Fig. 2.** Artist's rendition of abdominal aortic aneurysm illustrating side branches, aneurysm, and proximal and distal neck. On **left**, measurements as performed externally, on **right**, measurements with IVUS. Intraluminal line represents ultrasound catheter.

**Histologic evaluation.** Immediately after the IVUS examination was performed, the aortic specimens were fixed under pressure (100 mm Hg) in 10% buffered formalin for 2 hours. The distance between the aortic bifurcation and major side branches, that is, the celiac trunk, the superior and inferior mesenteric arteries, and the renal arteries, was measured externally, as was the distance between consecutive major side branches. In a similar fashion, in aneurysmal aortas the length of the aneurysm and the length of the proximal and distal neck were measured (Fig. 2). The specimens were subsequently decalcified in a standard RDO solution (Apex Inc., Plainfield, Ill.) for 5 hours and were further processed for routine paraffin embedding. Transverse sections (5  $\mu$ m thick) were cut at 10 mm intervals for normal and atherosclerotic aortas and at 5 mm intervals for aneurysmal aortas. The sections were stained with elastic van Gieson and hematoxylin-eosin techniques.

**Qualitative data analysis.** IVUS images obtained were photographed at increments of 5 mm. For comparison with the corresponding histologic sections, data from the displacement-sensing device and anatomic markers such as side branches

were used. Aortic wall characteristics and lesion morphologic characteristics assessed with IVUS were verified with the corresponding histologic characteristics.

**Quantitative data analysis.** For each specimen a set of five infrarenal histologic sections and their corresponding IVUS cross-sections taken at increments of 2 cm were quantitatively analyzed. Because the histologic sections did not maintain a circular shape as a result of the processing procedure, the lumen diameter was calculated from the lumen circumference both on histologic evaluation and IVUS. For this purpose a digital video analyzing system was used.<sup>14</sup> Distances between the major side branches and the aortic bifurcation measured externally along the central axis of the vessel with the use of a pair of compasses were compared with the distances measured with IVUS. The caudal borders of the side branches and the border of the aortic bifurcation were used as a reference (Fig. 2). Furthermore the distances between consecutive major side branches measured externally and with IVUS were compared, as were the length of the aneurysm and the length of the proximal and the distal neck. The proximal neck was defined as the distance between the caudal border of the most distal renal artery and the cranial border of the aneurysm; the distal neck was defined as the distance between the caudal border of the aneurysm and the aortic bifurcation (Fig. 2). Measurements of the length of the aneurysm and the proximal and distal neck were compared together because of the small number of measurements.

**Three-dimensional analysis.** To create a 3D model of the aorta the IVUS images were digitized at a resolution of  $800 \times 600 \times 8$  bits by a frame grabber (DT-3852) and aligned and stacked longitudinally.<sup>15,16</sup> Up to 200 images were acquired with a given interval (0.5 to 1.0 mm). In the resulting model two planes parallel to the linear axis of the vessel were selected to create longitudinal images that displayed the position and size of the aneurysm in relation to major side branches and aortic bifurcation.

**Statistical analysis.** Diameter and axial measurements obtained from aortic specimens and IVUS were compared with linear regression analysis and with the paired sample *t* test. A *p* value less than 0.05 was considered statistically significant.

## RESULTS

**Qualitative analysis.** A total of 285 IVUS cross-sections were matched with histologic sections for qualitative analysis. IVUS identified normal and ath-

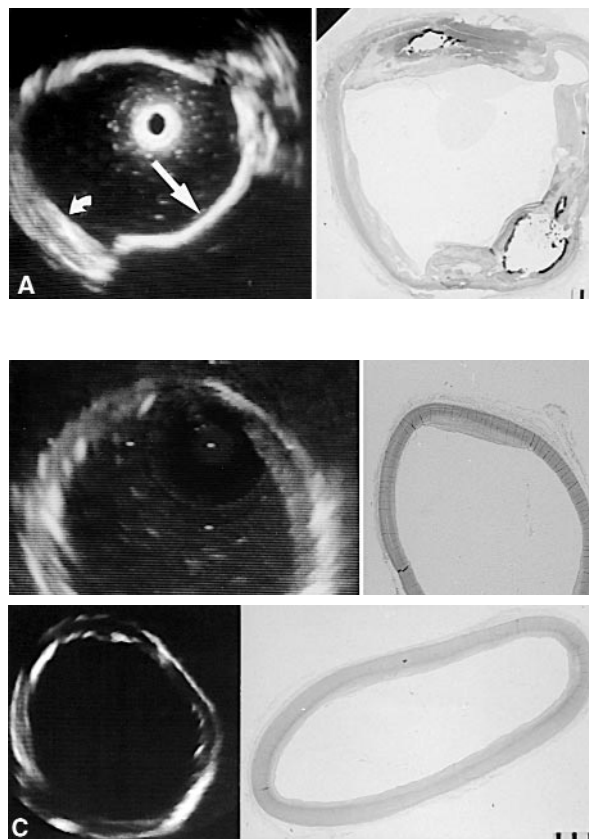


**Fig. 3.** Intravascular ultrasound cross sections and histologic counterparts (hematoxylin-eosin stain). **Upper panel** shows normal aorta with two-layered structure. **Middle panel** shows normal aorta with three-layered structure. **Lower panel** shows atherosclerotic aorta with calcified lesion at 4 o'clock position (*straight arrow*) and fibrous lesion at 8 o'clock position (*curved arrow*). Note absence of circular shape in histologic section in middle panel. Calibration: 5 mm (IVUS) and 1 mm (histologic evaluation).

erosclerotic vessel wall as a two- or three-layered structure (Fig. 3). In a two-layer structure the inner, less echogenic layer corresponded with intima and media; the outer hyperechoic layer corresponded with the adventitia. When a three-layered aspect was encountered, the intima appeared as a hyperechoic layer on the inside, the adventitia as an echo-bright layer on the outside, and the media as a hypoechoic layer between the intima and adventitia (Fig. 3).

In the presence of a lesion IVUS was able to distinguish fibrous lesions from calcified lesions. Fibrous lesion appeared as an echogenic structure through which the underlying wall was visible; calcified lesion was seen as a hyperechoic structure with peripheral shadowing preventing visualization of the

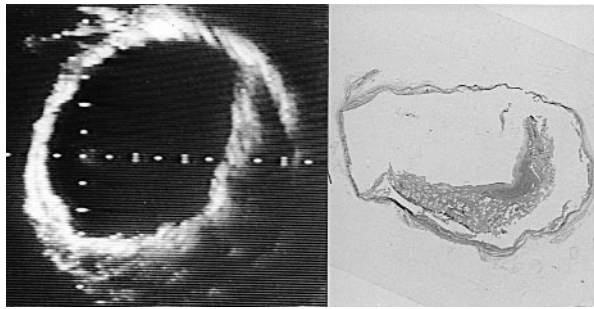


**Fig. 4.** Intravascular ultrasound cross section and histologic counterpart (hematoxylin-eosin stain) of aneurysmal aorta showing thrombus from 1 o'clock position to 7 o'clock position. Calibration: 5 mm (IVUS) and 1 mm.

vessel wall (Fig. 3). Thrombus, seen in three out of five aneurysms, was identified as a hypoechoic structure attached to the arterial wall (Fig. 4). Because the thrombotic lesions attenuated rather than reflected the signal, thrombus was distinguished from the echogenic reflection observed in fibrous lesions and the hyperechoic reflection with shadowing in calcified lesions. The two- or three-layered aspect of the aortic wall disappeared in the aneurysmal part of the aortas, although microscopy revealed a very thin media to be present in all histologic sections. Side branches were seen with IVUS as a distinct interruption of the vessel wall. Besides major side branches, small side branches (lumbar arteries) could be identified as well.

**Quantitative analysis.** Lumen diameter was assessed in 66 histologic and IVUS cross-sections; in 9 histologic sections lumen diameter could not be assessed because of damage incurred during histologic processing. Comparison between histologic evaluation and IVUS on lumen diameter showed a high correlation ( $r = 0.93$ ,  $p < 0.001$ , Fig. 5). Histologic lumen diameters were consistently smaller (17%) than the corresponding diameters measured with IVUS (mean difference,  $-3.1 \pm 2.0$  mm,  $p < 0.001$ ).

A total of 56 major side branches could be identified. Fifteen side branches were absent in the studied specimens, and the inferior mesenteric artery was not identified with IVUS in four instances; in three instances an aneurysmal aorta was involved, and in one an atherosclerotic aorta was involved. Measurements of the distance of the major side branches in relation to the aortic bifurcation obtained externally correlated well with IVUS measurements ( $r = 0.99$ ,  $p < 0.001$ , Fig. 5). External measurements were larger than those obtained with IVUS; the mean difference between both groups was significant ( $0.32 \pm$

$0.45$  cm,  $p < 0.001$ ). The distance between the consecutive side branches showed a high correlation ( $r = 0.99$ ,  $p < 0.001$ , Fig. 5) with no significant difference (mean difference of  $0.03 \pm 0.34$  cm,  $p = 0.59$ ). Measurements of the length of the aneurysm and the proximal and distal neck showed a high correlation ( $r = 0.99$ ,  $p < 0.001$ , Fig. 5) with a mean difference of  $0.06 \pm 0.15$  cm ( $p = 0.22$ ). The proximal neck was present in all specimens, and the distal neck was present in two specimens.

**Three-dimensional reconstruction.** In the longitudinal images derived from 3D analysis, the major side branches and the aneurysm were manifest (Fig. 6). The longitudinal image positioned through the renal arteries and the aortic bifurcation displayed the aneurysm and the proximal and distal neck. Compared with the single tomographic images, the transition from nonaneurysmal to aneurysmal aorta was better appreciated in the longitudinal (3D) reconstructions.

## DISCUSSION

With the introduction of the endovascular treatment of abdominal aortic aneurysms, new demands are being made on vascular surgeons and interventional radiologists. The success and safety of this new form of treatment require accurate and detailed preoperative and intraoperative visualization of the abdominal aorta and its side branches and characteristic features of the aneurysm.<sup>17</sup>

Techniques such as angiography and contrast computed tomography (CT) scanning have been used so far to evaluate the anatomic characteristics of aortic aneurysm.<sup>18,19</sup> Angiography, however, outlines only the vessel lumen and fails to show the outline of the aneurysm, the presence of thrombus, and the precise relation of the aneurysm to the side branches, thereby failing to define the length of the proximal and distal neck.

CT scanning, on the other hand, provides all the aforementioned information on aneurysms but provides little information on vessel wall condition and cannot be used during the intervention.<sup>20</sup>

Recently IVUS was recognized to determine luminal morphologic characteristics, to quantitate dimensions for device sizing, and to ensure secure device placement at the time of intervention.<sup>21-23</sup> White et al.<sup>21</sup> reported a single patient study in which preoperative IVUS compared with CT scanning in abdominal aortic aneurysm was capable of providing accurate information on aortic wall characteristics and on the position of the visceral and renal arteries in relation to the aneurysm. Verbin et

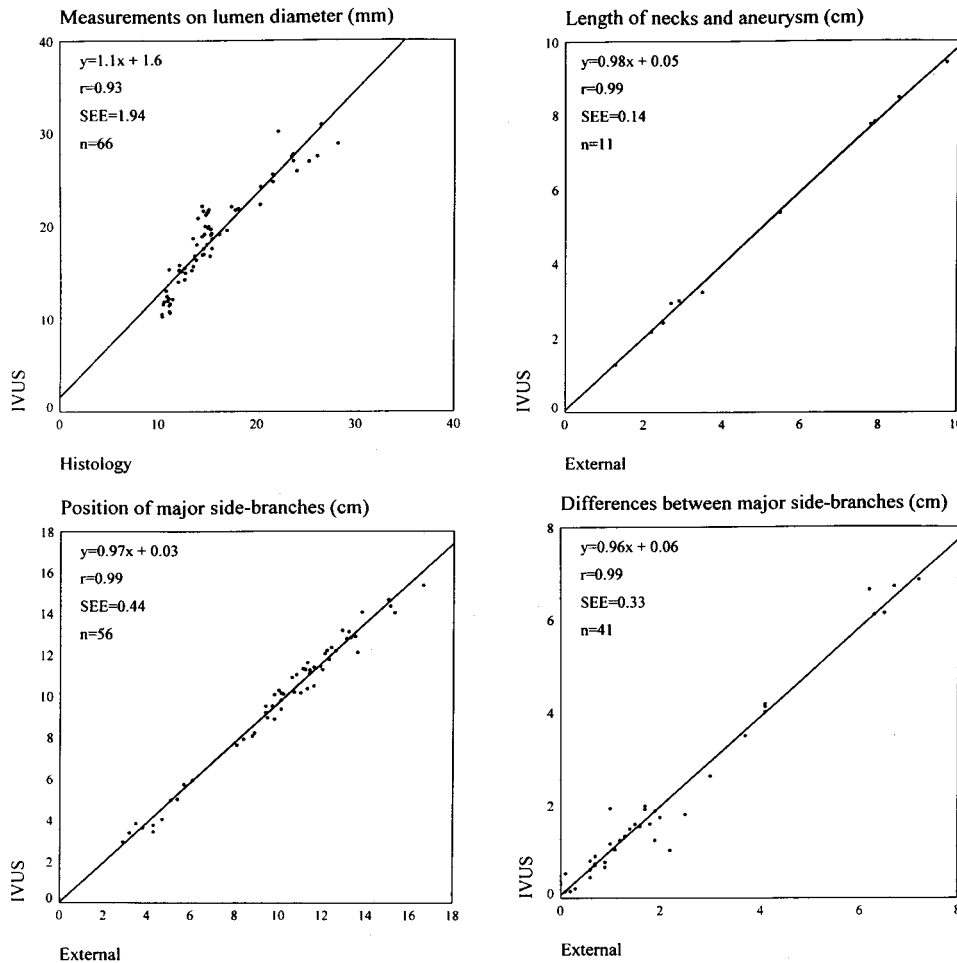
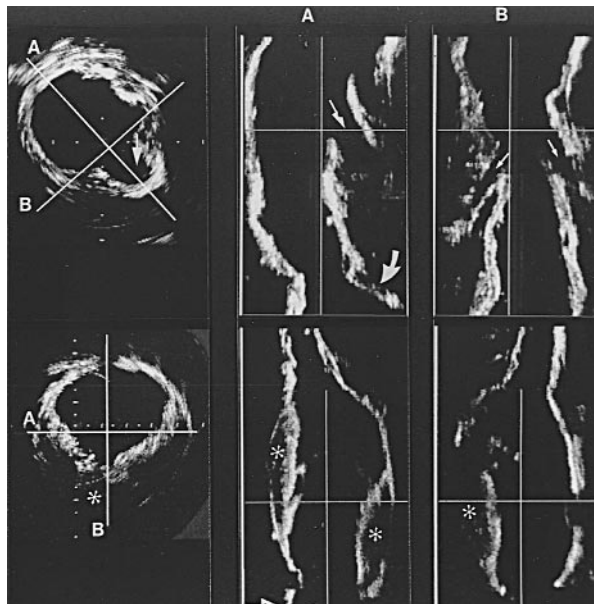


Fig. 5. Comparison between histologic and external measurements and intravascular ultrasound measurements.

al.<sup>22</sup> demonstrated that IVUS used in normal and aneurysmal canine aortas after stent graft placement could identify stent-aorta interfaces, thrombus formation, and graft folding, characteristics missed by angiography and postinterventional CT scanning. Lyon et al.<sup>23</sup> reported on the clinical use of IVUS in endovascular procedures. IVUS was found to be more sensitive in detecting major arterial and graft lesions, which could result in graft thrombosis or technical failure, than intraoperative angiography. IVUS, however, was less sensitive in detecting endoleaks than postoperative CT.

This validation study performed in vitro demonstrates the capacity of IVUS to identify the different morphologic and quantitative characteristics of normal, atherosclerotic, and aneurysmal aorta. A distinction could be made between fibrous and calcified lesion and thrombus that allows definition and characterization of the proximal and distal neck. This information might be valuable during the endovas-

cular treatment of patients with abdominal aortic aneurysms. The comparison between histologic evaluation and IVUS on lumen diameter and axial measurements showed a high correlation. The observation that lumen diameter in the histologic sections was smaller than in the IVUS cross-sections was attributed to shrinkage of histologic specimens during fixation, a process also observed by other investigators.<sup>24</sup> The observation that the distance between major side branches and aortic bifurcation was larger (0.3 cm) on external measurements than that measured with IVUS can be ascribed to the curved nature of the pullback of the ultrasound catheter (Fig. 2). This assumption is supported by the finding that no significant difference was observed in the distance between the consecutive major side branches where no curvature occurred. More important, the length of the aneurysm and the length of the proximal and distal neck were adequately assessed with IVUS.



**Fig. 6.** Three-dimensional reconstruction of aneurysmal aorta. Lines A and B represent longitudinal reconstructed sections (**right panels**), which stand perpendicular to each other as demonstrated in axial image (**left panel**). **Upper panel** shows proximal neck with superior mesenteric artery (*large arrow*), renal arteries (*small arrows*), and proximal part of aneurysm (*curved arrow*). **Lower panel** shows proximal neck, aneurysm with thrombus (\*), and aortic bifurcation (*open arrow*).

The 3D reconstructions and longitudinal images enhance the spatial insight in the aneurysm. The perpendicular cuts show a better continuity between the consecutive images and therefore have an additional value in the interpretation of IVUS images. Similarly, White et al.<sup>21</sup> reported that 3D IVUS imaging facilitated interpretation of the tomographic images.

Because of the results of this study and the high costs of IVUS catheters, we believe that in the future IVUS should be used during the endovascular treatment of patients with abdominal aortic aneurysm and not as a diagnostic device before intervention only. Immediately before stent graft placement IVUS will be able to assess the relevant quantitative parameters of the aneurysm; after intervention IVUS can be used to document position and deployment of the stent graft. Additional interventions may be performed during the same session based on information obtained with IVUS. These features give IVUS a head start, because neither angiography nor CT scanning can supply all the necessary information on the position and deployment of the stent graft during intervention. IVUS would be the most

appropriate choice for interventional imaging.

It should be acknowledged that the number of aneurysmal specimens studied was limited and that the aneurysms studied were not suspected on clinical evaluation. Three of the aneurysms were smaller than 5 cm. In addition, this study was performed without pulsatile blood flow; its presence may have consequences on the quality of 3D reconstruction.

## CONCLUSION

IVUS provides accurate information on vessel wall and lesion morphologic characteristics of the abdominal aorta. The precise identification of the major side branches, aortic bifurcation, and aneurysm allows accurate assessment of the length of the aneurysm and the proximal and distal neck. 3D reconstruction facilitates spatial insight in the aneurysm and surrounding vascular structures.

We thank H. van Seyen and G. Verheyen for their support in harvesting the aortic specimens. We thank Dr. R. Berger for supplying the HP IVUS system.

## REFERENCES

1. Balko A, Piasecki GJ, Shah DM, Carney WI, Hopkins RW, Jackson BT. Transfemoral placement of intraluminal polyurethane prosthesis for abdominal aortic aneurysm. *J Surg Res* 1986;40:305-9.
2. Mirich D, Wright KC, Wallace S, Yoshioka T, Lawrence DD, Charnsangavej C, et al. Percutaneously placed endovascular grafts for aortic aneurysms: feasibility study. *Radiology* 1989;170:1033-7.
3. Parodi JC, Palmaz JC, Barone HD. Transfemoral intraluminal graft implantation for abdominal aortic aneurysms. *Ann Vasc Surg* 1991;5:491-9.
4. Lazarus HM. Endovascular grafting for the treatment of abdominal aortic aneurysms. *Surg Clin North Am* 1992;72:959-68.
5. Chuter TAM, Green RM, Ouriel K, Fiore WM, DeWeese JA. Transfemoral endovascular aortic graft placement. *J Vasc Surg* 1993;18:185-97.
6. Moore WS, Vescera CL. Repair of abdominal aortic aneurysm by transfemoral endovascular graft placement. *Ann Surg* 1994;220:331-41.
7. Parodi JC. Endovascular repair of abdominal aortic aneurysms and other arterial lesions. *J Vasc Surg* 1995;21:549-55.
8. Balm R, Eikelboom BC, May J, Bell PRF, Swedenborg J, Collin J. Early experience with Transfemoral Endovascular Aneurysm Management (TEAM) in the treatment of aortic aneurysms. *Eur J Vasc Endovasc Surg* 1996;11:214-20.
9. Blum U, Voshage G, Lammer J, Beyersdorf F, Töllner D, Kretschmer G, et al. Endoluminal stent-grafts for infrarenal abdominal aortic aneurysms. *N Engl J Med* 1997;336:13-20.
10. Losordo DW, Rosenfield K, Pieczek A, Baker K, Harding M, Isner JM. How does angioplasty work? Serial analysis of human iliac arteries using intravascular ultrasound. *Circulation* 1992;86:1845-58.
11. Gussenhoven EJ, Lugt van der A, Pasterkamp G, Berg van

- der FG, Sie LH, Vischjager M, et al. Intravascular ultrasound predictors of outcome after peripheral balloon angioplasty. *Eur J Vasc Endovasc Surg* 1995;10:279-88.
12. Lugt van der A, Gussenhoven EJ, Stijnen T, Strijen van M, Driel van E, Egmond van FC, et al. Comparison of intravascular ultrasonic findings after coronary balloon angioplasty evaluated in vitro with histology. *Am J Cardiol* 1995;76:661-6.
  13. Gussenhoven EJ, Lugt van der A, Strijen van M, Li W, Kroeze H, The SHK, et al. Displacement sensing device enabling accurate documentation of catheter tip position. In: Roelandt J, Gussenhoven EJ, Bom N, editors. *Intravascular ultrasound*. Dordrecht: Kluwer Academic Press; 1993. p. 157-66.
  14. Wenguang L, Gussenhoven WJ, Zhong Y, The SHK, Di Mario C, Madretsma S, et al. Validation of quantitative analysis of intravascular ultrasound images. *Int J Card Imaging* 1991;6:247-53.
  15. Li W, Bom N, Egmond van FC. Three-dimensional quantification of intravascular ultrasound images. *J Vasc Invest* 1995;1:57-61.
  16. Wenguang L, Bom N, Birgelen von C, Steen van der TFW, Korte de CL, Gussenhoven EJ, et al. State of the art in ICUS quantitation. In: Reiber JHC, Wall van der EE, editors. *Cardiovascular imaging*. Dordrecht: Kluwer Academic Publishers; 1996. p. 79-82.
  17. Moritz JD, Rotermund S, Keating DP, Oestmann JW. Infrarenal abdominal aortic aneurysms: implications of CT evaluation of size and configuration for placement of endovascular aortic grafts. *Radiology* 1996;198:463-6.
  18. Rubin GD, Walker PJ, Dake MD, Napel S, Jeffrey B, McDonnell CH, et al. Three-dimensional spiral computed tomographic angiography: an alternative imaging modality for the abdominal aorta and its branches. *J Vasc Surg* 1993;18:656-65.
  19. Siegel CL, Cohan RH. CT of abdominal aortic aneurysms. *AJR* 1994;163:17-29.
  20. Balm R, Kaatee R, Blankensteijn JD, Mali WPTM, Eikelboom BC. CT-angiography of abdominal aortic aneurysms after transfemoral endovascular aneurysm management. *Eur J Vasc Endovasc Surg* 1996;12:182-8.
  21. White RA, Scocciati M, Back M, Kopchok G, Donayre C. Innovations in vascular imaging: arteriography, three-dimensional CT scans, and two- and three-dimensional intravascular ultrasound evaluation of an abdominal aortic aneurysm. *Ann Vasc Surg* 1994;8:285-9.
  22. Verbin C, Scocciati M, Kopchok G, Donayre C, White RA. Comparison of the utility of CT scans and intravascular ultrasound in endovascular aortic grafting. *Ann Vasc Surg* 1995;9:434-40.
  23. Lyon RT, Veith FJ, Berdejo GL, Okhi T, Sanchez LA, Wain RA, et al. Utility of intravascular ultrasound for assessment of endovascular procedures. Presented at the Joint Annual Meeting for the Society for Vascular Surgery and North American Chapter, International Society for Cardiovascular Surgery; 1997. p. 43.
  24. Gussenhoven EJ, Lugt van der A, Steen van der AFW, Ligtvoet KM. What have we learned from in vitro intravascular ultrasound? *Am Heart J* 1996;132:702-10.

Submitted July 7, 1997; accepted Sept. 17, 1997.